Curing Behavior and Thermal Properties of Multifunctional Epoxy Resin with Methylhexahydrophthalic Anhydride

Yanfang Liu,[1,2] Zhongjie Du,[1] Chen Zhang,[1] Congju Li,[3] Hangquan Li[1]

[1]*The Key Laboratory of Beijing City on Preparation and Processing of Novel Polymer Materials, Beijing University of Chemical Technology, Beijing 100029, China*
[2]*College of Chemistry and Environmental Science, Hebei University, Baoding 071002, China*
[3]*Beijing Key Laboratory of Clothing Material R&D and Assessment, Beijing Institute of Clothing Technology, Beijing 100029, China*

Received 22 February 2006; accepted 13 August 2006
DOI 10.1002/app.25291
Published online in Wiley InterScience (www.interscience.wiley.com).

ABSTRACT: The curing behavior and thermal properties of bisphenol A type novolac epoxy resin (bisANER) with methylhexahydrophthalic anhydride (MHHPA) at an anhydride/epoxy group ratio of 0.85 was studied with Fourier-transform infrared (FTIR) spectroscopy, differential scanning calorimetry (DSC), and thermogravimetry. The results showed that the FTIR absorption intensity of anhydride and epoxide decreased during the curing reaction, and the absorption peak of ester appeared. The dynamic curing energies were determined as 48.5 and 54.1 kJ/mol with Kissinger and Flynn–Wall–Ozawa methods, respectively. DSC measurements showed that as higher is the curing temperature, higher is the glass transition. The thermal degradation of the cured bisANER/MHHPA network was identified as two steps: the breaking or detaching of $-OH$, $-CH_2-$, $-CH_3$, $OC-O$ and $C-O-C$, etc., taking place between 300 and 450°C; and the carbonizing or oxidating of aromatic rings occurring above 450°C. The kinetics of the degradation reaction was studied with Coats–Redfern method showing a first-order process. In addition, vinyl cyclohexene dioxide (VCD) was employed as a reactive diluent for bisANER (VCD/bisANER = 1 : 2 w/w) and cured with MHHPA, and the obtained network had a higher T_g and a slight lower degradation temperature than the undiluted system. © 2006 Wiley Periodicals, Inc. J Appl Polym Sci 103: 2041–2048, 2007

Key words: composites; curing of polymers; degradation; glass transition; kinetics (polymer); matrix; resins

INTRODUCTION

Epoxy resins are the most important class of matrices for polymer composites due to their high mechanical strength, good thermal, electrical, and chemical resistance. The curing reaction mechanism, thermal and mechanical properties of epoxy resins depend on their physical and chemical natures. Therefore, considerable attention has been paid to the curing reaction, thermal and mechanical properties of epoxy resins.[1–14] However, the main research works were focused on the systems based on bifunctional epoxy resins[1–10] and tetrafunctional epoxy resins,[10–14] with various curing agents; few efforts was made on those involving multifunctional novolac epoxy resins.

Bisphenol A type novolac epoxy resin (bisANER) is a high-functionality solid polymeric epoxy resin, and has been employed as the matrix for high performance fiber-reinforced composites in the aerospace industry and as encapsulant for electronic components.[15–17] The preparation of bisANER and the curing reaction with 4,4′-diaminodiphenyl sulfone was reported in our previous work,[18] and the prepared products were mainly consisted of trimers and dimers.

In some applications requiring low viscosity epoxy resins systems, bisANER can be diluted with some diluents or cured with some liquid curing agent to decrease the viscosity of the system. Vinyl cyclohexene dioxide (VCD) is a cycloaliphatic epoxide with low viscosity, good heat resistance, superior mechanical and electrical properties,[19] and can be used as a reactive diluent. For the curing agents, methylhexahydrophthalic anhydride (MHHPA) is a liquid agent with low viscosity and can cured with epoxy resins to produce transparent products used as the matrix for many advanced materials in the aerospace and electronic industries. But the curing reaction mechanism of epoxy resin with MHHPA and the properties of the cured product are different with aromatic diamine.

In this study, the curing behavior and thermal properties for bisANER with or without VCD through MHHPA was studied using differential scanning cal-

Correspondence to: H. Li (hli45@yahoo.com.cn).
Contract grant sponsor: National Natural Science Foundation of China; contract grant number: 50503001.
Contract grant sponsor: Beijing National Natural Science Foundation; contract grant number: KZ200510012010.

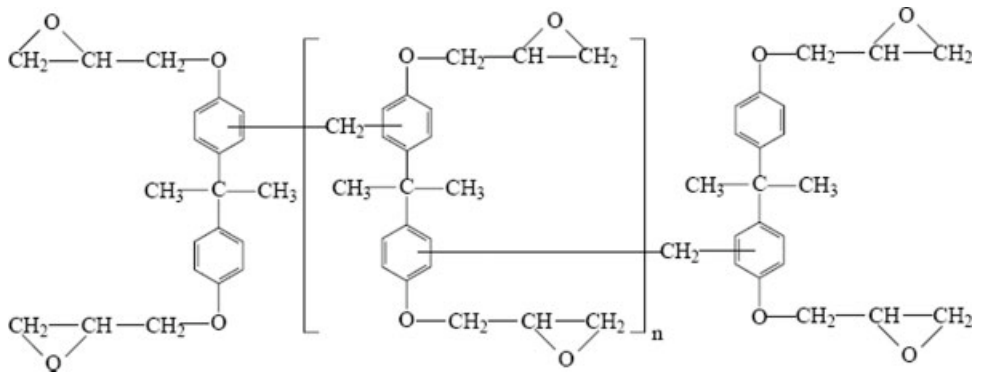

Scheme 1 Molecular structure of bisANER.

orimetry (DSC), Fourier-transform infrared (FTIR) spectroscopy, and thermogravimetry.

EXPERIMENTAL

Materials and sample preparation

Bisphenol-A, formaldehyde (37% aqueous), and *n*-butanol were from Beijing Chemical (China). Epichlorohydrin, oxalic acid, sodium hydroxide, and benzene were from Tianjin Chemical (China). Tetrabutylammonium bromide was from Shanghai Chemical (China). MHHPA was from Wuxi Wells synthetic material (China). VCD was from Sigma-Aldrich Chemie (Switzerland). All solvents were used as received without further purification.

BisANER was synthesized according to the literature,[18] and its structure was shown in Scheme 1. The epoxy equivalent weight (EEW) of the synthesized bisANER is 213 g/eq, which was determined with the hydrochloric acid–acetone titration method.[20] Based on the determined EEW value, the bisANER and MHHPA were mixed at the 1 : 0.85 stoichiometric ratio of epoxide to anhydride groups. In addition, bisANER and VCD were mixed at a weight ratio of 2 : 1; subsequently, the mixture was mixed with MHHPA at a 1 : 0.85 stoichiometric ratio of epoxide to anhydride groups.

The mixtures were subjected to the following curing programs (1) bisANER/MHHPA mixtures were first cured at 140°C for 1 h, then cured at 180 and 200°C, respectively, for different periods. (2) bisANER/VCD/MHHPA mixtures were first cured at 140°C for 1 h, and then cured at 180°C for different periods.

FTIR measurements

A Nicolet Nexus 670 FTIR spectrometer was used to determine the structural changes of the bisANER/MHHPA during the curing and thermal degradation reactions. The sample was coated onto a potassium bromide plate as a thin film at room temperature. For monitoring curing, the coated film was placed in an oven at 180°C and retrieved at certain time interval for scanning. For studying the thermal degradation, the sample cured at 180°C for 8 h was heated in an oven and at 10°C/min and retrieved for scanning at certain temperatures.

DSC measurements

A PerkinElmer Pyris1 differential scanning calorimeter was used to determine the curing behavior and the glass transition temperatures (T_gs) of bisANER/MHHPA, operating in dynamic nitrogen atmosphere at a flowing rate of 40 mL/min.

BisANER/MHHPA mixtures (about 6.5 mg each) was subjected to dynamic DSC scans at heating rates of 5, 7.5, 10, 12.5, and 15°C/min, respectively, to determine the dynamic curing behavior. In addition, about 16 mg of cured sample was placed in a sample cell, and then the sample was subjected to a dynamic DSC scan at 20°C/min to determine the T_g. The glass transition process appears as baseline shift, and the T_g is taken as the midpoint of the heat capacity change (ΔC_p).

TGA–DSC measurements

A Netzsch STA 449C TG-DSC simultaneous analyzer was used to determine the weight loss and heat release behaviors of bisANER/MHHPA and bisANER/VCD/MHHPA during the degradation process. About 16 mg of cured sample was placed on the instrument, and then was heated to 700°C at a heating rate of 10°C/min. The experiments were carried out under dynamic air at a flowing rate of 20 mL/min.

RESULTS AND DISCUSSION

FTIR study of curing reaction

The curing reaction of the epoxy–anhydride in the presence of OH groups was first initiated by the addi-

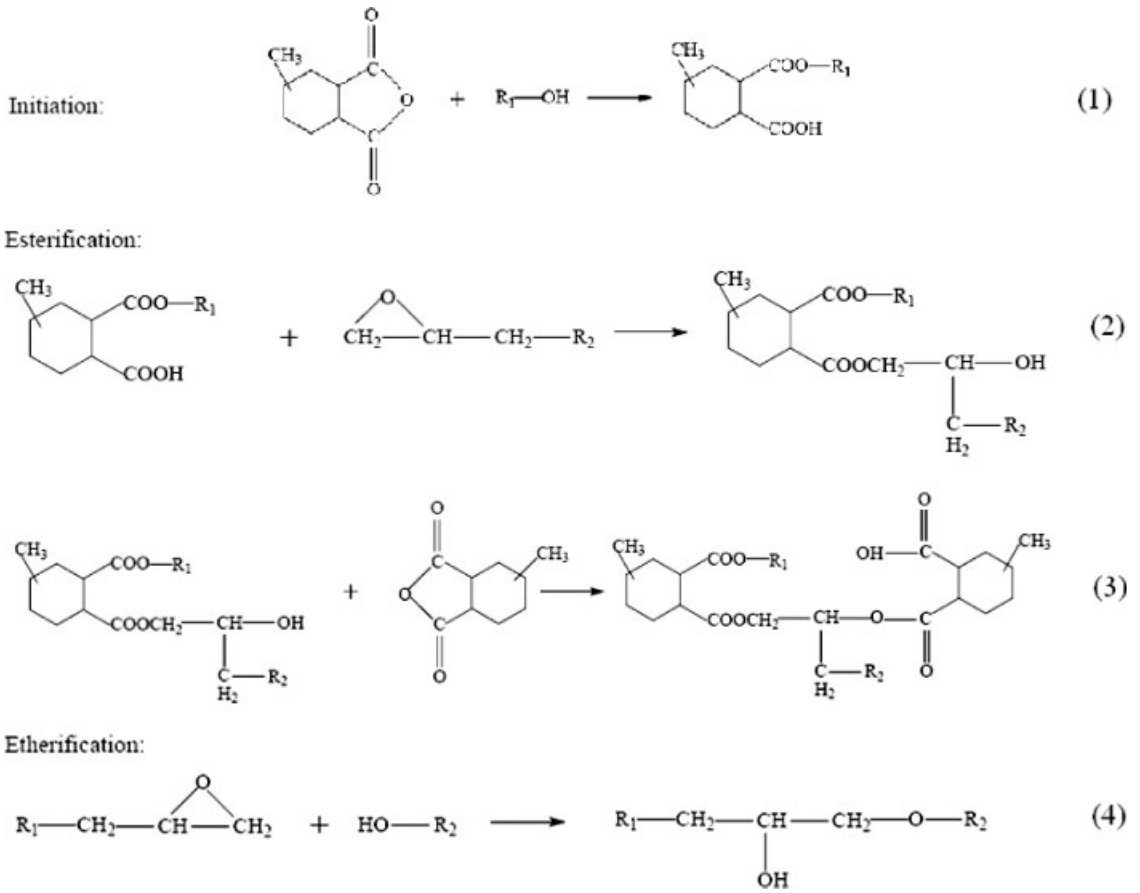

Scheme 2 The curing reaction scheme for epoxy resin with MHHPA.

tion of hydroxyl groups on the epoxy resins onto the anhydride ring generating an ester group and a carboxylic acid group. The newly formed carboxyl group reacted quickly with another epoxy group and formed an additional ester and a hydroxyl group. In addition, the reaction between the hydroxyl and epoxy group occurred as a side reaction during the curing, especially at higher temperatures. Therefore, esterification and etherification were the main curing reactions. The curing mechanisms are sketched in Scheme 2.[21–24]

Figure 1 presents the FTIR spectra of the bisANER/MHHPA system during the curing reaction. The assignments of the absorption features are as follows:[25,26] 3700–3320 cm^{-1} to hydroxyl groups, 2955–2869 cm^{-1} to the CH_3 and CH_2, 1860 and 1785 cm^{-1} to anhydride C=O, 1700 cm^{-1} to carboxylic acid C=O, 1731 cm^{-1} to ester linkage C=O, 1610, 1506, and 1455 cm^{-1} to the stretching and deformation aromatic C=C, 1247 cm^{-1} to the aromatic ether ϕ—O—C, 1108 and 1038 to the deformation of the aromatic CH, 944 and 901 cm^{-1} to the pathalic anhydride C—O, the stretching of C—O—C on epoxide also occurs in this region but cannot be clearly discerned in the uncured resin system, 913 cm^{-1} to epoxide groups, 830 cm^{-1} to the out-of-plane deformation of the aromatic CH, 750 and 624 cm^{-1} to the out-of-plane deformation of the phthalic anhydride C—H and C—C—C.

The structural changes during curing process can be identified from Figure 1. After cured at 180°C for 30 min, the absorption intensity of hydroxyl with the broad spectral feature increased, while the absorption of C=O of anhydride at 1858 cm^{-1} disappeared completely and at 1785 cm^{-1} decreased greatly. Correspondingly, the absorption intensity of the C=O in the newly formed ester linkage at 1731 cm^{-1} appeared and became stronger. The above-mentioned changes were attributed to the reaction of anhydride with a hydroxyl forming a carboxylic acid, which in turn caused the ring-opening of an epoxide group generating an additional hydroxyl moiety. As a result, the absorption intensity of epoxide groups, which was swamped by the pathalic anhydride C—O peak at 901 cm^{-1}, decreased. With the proceeding of curing reaction, the absorption intensity at 913 cm^{-1} decreased gradually and the absorption peak disappeared completely after 8 h at 180°C. Moreover, it can be seen that the absorption intensity of epoxide groups decreased slowly with increasing time at later curing stage, which indicated that the reaction rate decreased gradually with the reaction proceeding. In

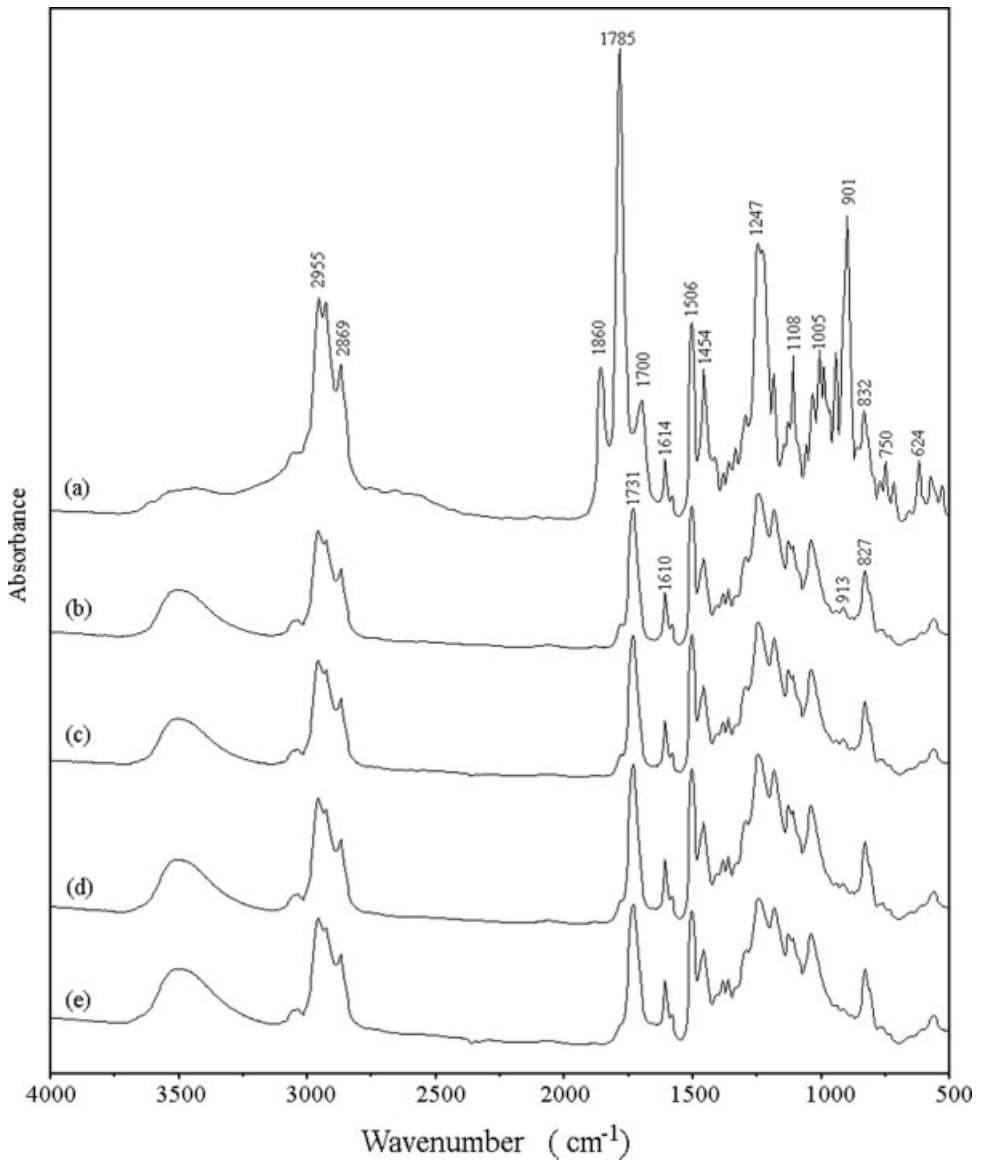

Figure 1 FTIR spectra of bisANER/MHHPA uncured (a) and cured at 180°C for (b) 30 min; (c) 90 min; (d) 240 min, and (e) 480 min.

addition, the absorption of 750 and 624 cm^{-1} disappeared after 30 min, indicating that most of phthalic anhydrides had been consumed.

Curing kinetics

The curing reaction kinetic parameters can be evaluated with a multiple-heating-rate method by determining the exothermic peak temperatures at several heating rates. In practice, two convenient multiple-heating-rate methods are generally used. One is the maximum reaction rate method proposed by Kissinger,[27] which is based on the fact that the exothermic peak temperature (T_p) varies with the heating rates. The other is the isoconversion method proposed by Flynn, Wall,[28] and Ozawa,[29] which is based on the fact that isoconversion can be reached at different temperatures with various heating rates.

Kissinger's approach assumes that the maximum reaction rate occurs at peak temperatures, where $d^2\alpha/dt^2$, it can be expressed as

$$\ln\left(\frac{\beta}{T_p^2}\right) = \ln\left(\frac{AR}{E}\right) - \frac{E}{RT_p} \quad (1)$$

where β is the linear heating rate, A is the pre-exponential factor, E is the activation energy, and R is the universal gas constant. Therefore, a plot of $\ln(\beta/T_p^2)$ versus $1/T_p$ gives the values of E and A.

Flynn–Wall–Ozawa method assumes that the degree of conversation at peak temperatures for different heating rates is constant. It can be expressed as

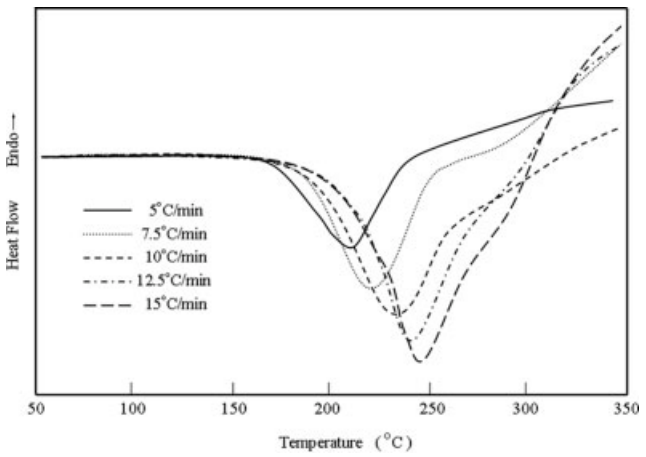

Figure 2 Dynamic curing DSC curves of bisANER/MHHPA.

$$\log \beta = -\frac{0.4567E}{RT} + C \tag{2}$$

where C is a constant, T is the isoconversion temperature, and other parameters are the same as described earlier. Plotting log β versus $1/T_p$, the activation energy can be obtained from the slope.

In Figure 2, the heat flow was plotted as a function of the temperature for five different heating rates. It is seen that the exothermic reaction proceeded in a wide temperature range, and the maximum rate temperatures of the curing reaction increased with increasing heating rate. All the exothermic peak temperatures (T_p) of the DSC curves at different heating rates were listed in Table I, and the curing kinetic parameters determined by the Kissinger and Flynn–Wall–Ozawa methods were also summarized in Table I. The value of the curing active energy is lower than the bisANER with 4,4′-diaminodiphenyl sulfone.[18]

Glass transition temperature and curing reaction process

T_g of an epoxy resin network is the reflection of the structure and curing extent for a given epoxy resin system. For this reason, the curing behavior in question was studied by monitoring the variation of T_g during the reaction process.

The T_g data measured with DSC for the bisANER/MHHPA and bisANER/VCD/MHHPA systems cured at various temperatures and time lengths were shown in Figure 3 and Table II. These data showed

TABLE I
The Peak Temperatures of DSC and the Kinetic Parameters of the Dynamic Curing of the BisANER/MHHPA

Heating rates (°C/min)	T_p (°C)	Kissinger		Flynn–Wall–Ozawa
		E (kJ/mol)	A (s^{-1})	E (kJ/mol)
5	209.3	48.5	23.1	54.1
7.5	220.8			
10	234.8			
12.5	243			
15	247.5			

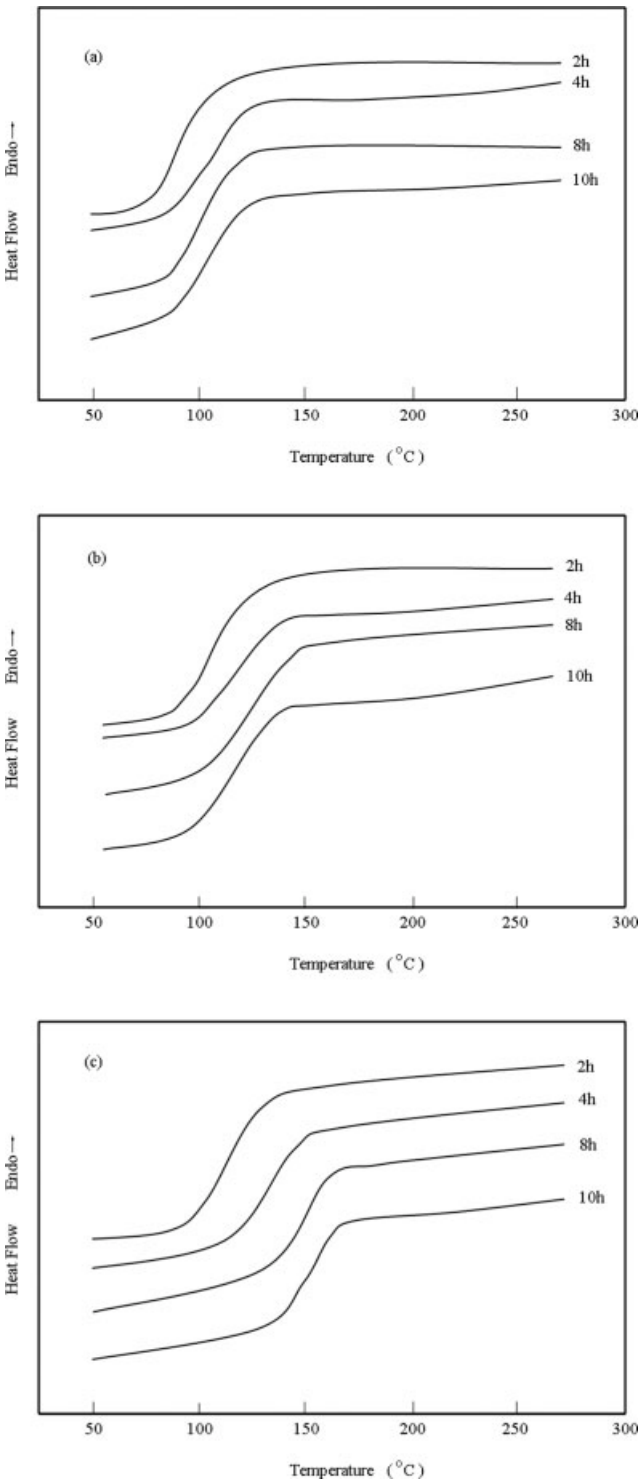

Figure 3 DSC curves of (a) bisANER/MHHPA cured at 180°C, (b) bisANER/MHHPA cured at 200°C, and (c) bisANER/VCD/MHHPA cured at 180°C for different periods.

TABLE II
Glass Transition Temperature (°C) of the BisANER/MHHPA and BisANER/VCD/MHHPA Networks Cured at Different Conditions

Curing time (h)	1	2	4	8	10
BisANER/MHHPA					
180°C	71.3	91.1	105.4	105.7	106.4
200°C	75.8	99.4	109.3	119.1	119.5
BisANER/VCD/MHHPA					
180°C	115.1	120.1	135.5	152.2	152.6

that the T_g of the two systems depended both upon cured temperature and time. At a given curing temperature, T_g increased with increasing curing time and leveled off to a certain value. On the other hand, at given curing time, higher curing temperature gave a higher T_g value. These changes of T_g reflected the segment movement in the network and the curing behavior. Within short curing time, both crosslinking degree and molecular weight were low, and the molecular movement was relatively easy, so the networks gave rise to a low T_g value. In this stage, the curing proceeded smoothly, and a higher curing temperature resulted in a higher curing rate. With increasing curing time, both crosslinking density and molecular weight increased, the segment movement became more difficult. When the curing reached a certain extent, the segment movements were greatly restricted and the curing could not proceed further, so the T_g of the network no longer changed. At higher curing temperature, the segments acquired greater energy, and a higher T_g was exhibited.

It can be seen from Figure 3 and Table II that the T_gs of the bisANER/VCD/MHHPA were obviously higher than those of bisANER/MHHPA. This indicated that VCD increased the restriction of the segments. As shown in Scheme 1, the backbone of the bisANER molecule was mainly composed of aromatic rings, and the movements of the bisANER segments needed more free volume than that of no-aromatic-ring molecules. Because of the steric hindrance, the bisANER segments could not penetrated into the free volume inside the network. However, the occupying space of VCD molecule is smaller than the bisANER, and the movements of VCD molecules may penetrate easier into the network and result in a higher crosslinking density. For this reason, the bisANER/VCD/MHHPA system gave rise to a higher T_g value than those of bisANER/MHHPA cured with the same condition.

Thermal degradation behavior

Figure 4 presents the FTIR spectra of bisANER/MHHPA during the thermal degradation process. When the degradation temperature reached 350°C, some changes in the structure of the bisANER/MHHPA can be read from the spectra, such as the absorption intensities at 3505, 2962–2867, 1733, 1506, 1183, 1126, and 1040 cm^{-1} were all weakened in some degree, which indicated that hydroxyl groups, alkyl groups, ester linkage, aromatic C=C, aromatic C—O and ether linkage were affected by the thermal energy, and some of these groups were broken. With rising degradation temperature, the absorption intensities within these regions decreased gradually. After the temperature exceeded 450°C, the absorption intensities at 3505, 2962–2867, 1733, 1458, 1247, and 827 cm^{-1} were weakened further, especially those at 2962–2867, 1733, and 827 cm^{-1}. These changes in characteristic features indicated that some groups were seriously broken, such as alkyl groups, ester linkage, aromatic C—O, and aromatic C—H. One may conclude that the degradation of bisANER/MHHPA may proceed in the following sequence: first involving the breaking, detachment, or oxidation of —OH, $—CH_2—$, $—CH_3$, OC—O, and C—O—C, and thereafter the carbonization and oxidation of aromatic rings.

Figure 5 shows the weight loss behavior from TGA of bisANER/MHHPA and bisANER/VCD/MHHPA networks in dynamic air atmosphere. From the curves, two stages of weight loss in dynamic air can be identified.

When the degradation temperature reached 350°C, weight loss of bisANER/MHHPA networks was about 5% while that of bisANER/VCD/MHHPA networks was about 15%, which corresponded to the breaking or detachment of —OH, $—CH_2—$, $—CH_3$, OC—O, and C—O—C, etc., as shown in Figure 4.

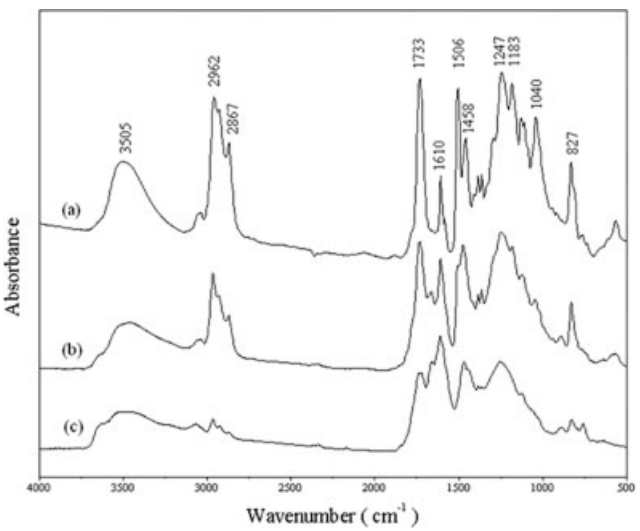

Figure 4 FTIR spectra of bisANER/MHHPA (a) cured at 180°C for 8 h and afterward heated to (b) 350°C and (c) 450°C at a heating rate of 10°C/min in static air atmosphere.

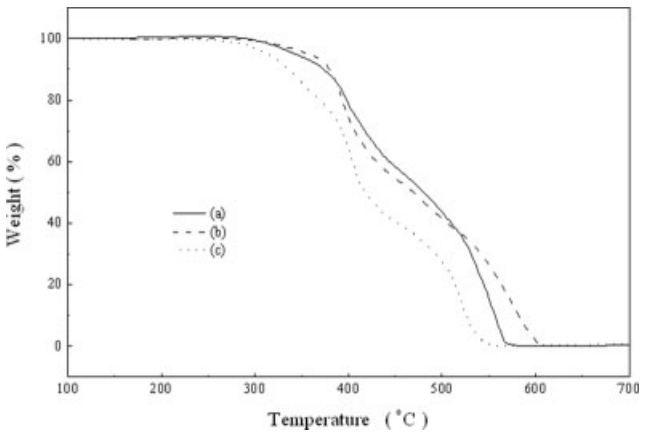

Figure 5 TGA curves at a heating rate of 10°C/min of (a) bisANER/MHHPA cured at 180°C, (b) bisANER/MHHPA cured at 200°C, and (c) bisANER/VCD/MHHPA cured at 180°C for 8 h.

With rising temperature, these groups were further broken and other links or groups were gradually degraded. When the temperature reached 450°C, weight loss of bisANER/MHHPA networks was about 43–46% while that of bisANER/VCD/MHHPA networks was about 60%. According to Figure 4, the subsequent reaction was mainly attributed to the breaking of —OH, —CH_2—, —CH_3, OC—O, and C—O—C, etc., and aromatic rings at higher temperatures. When temperature was above 450°C, the degradation reactions of bisANER/MHHPA and bisANER/VCD/MHHPA networks all proceeded into the second weight loss stage. In this stage, the residual groups or links of —OH, OC—O, and C—O—C were gradually broken or oxidated, and the main reactions were the carbonization and oxidation of aromatic rings.

In addition, the DSC curves in Figure 6 show the heat release behavior of cured samples during the thermal degradation process. Corresponding to the first weight loss stage, only a broad and low exothermal peak was given. This suggested that the breaking or detachment of —OH, —CH_2—, —CH_3, and C—O—C were hardly exothermic, some of which may be endothermic. However, in the higher degradation temperatures, a large peak was exhibited. Since the corresponding reactions were mainly oxidation, it was natural to release a large amount of heat.

From Figure 5, it can be seen that bisANER/VCD/MHHPA networks degraded at a slight lower temperature than bisANER/MHHPA. This can be explained from the molecular structure viewpoint. VCD is a cycloaliphatic diepoxide, and saturated carbon–hydrogen is the main structure character. After cured in the bisANER/VCD/MHHPA system, though VCD can increase the T_g of the networks, VCD are weaker points than that of the bisANER, and may be broken easier.

Thermal degradation kinetics

Kinetic information can be obtained from thermogravimetric experiments. To determine the kinetic parameters of the degradation from the thermogravimetric data, the first step is to evaluate the conversation of the reaction. In TGA dynamic experiments, the weight change of the sample is regarded as a function of temperature, and the conversation can be expressed as

$$\alpha = \frac{w_i - w_T}{w_i} \tag{3}$$

where w_i is the sample weight in i stage, w_T is the residual weight of the w_i at temperature T. Therefore, with the equation, the conversions are calculated for different degradation stages from the TGA curves.

To determine the kinetic parameters of the degradation process, many methods have been reported. Among them, Coats–Redfern used the following equation[30]

$$\ln\frac{g(\alpha)}{T^2} = \ln\left[\frac{AR}{\beta E}\left(1 - \frac{2RT}{E}\right)\right] - \frac{E}{RT} \tag{4}$$

where $g(\alpha)$ is a integral function of conversion dependence function. The correct form of $g(\alpha)$ depends on the proper mechanism of the decomposition reaction.[6] Different expressions of $g(\alpha)$ for some solid-state reaction mechanisms can be described as following: first order: $-\ln(1-\alpha)$; second order: $1/(1-\alpha)$; third order: $1/(1-\alpha)^2$. Based on the experimental data and according to eq. (4), the activation energy can be calculated from a fitting of $\ln(g(\alpha)/T^2)$ versus $1/T$ plots.

In this study, only conversions values in the range 5–20% were used. The results of the first degradation

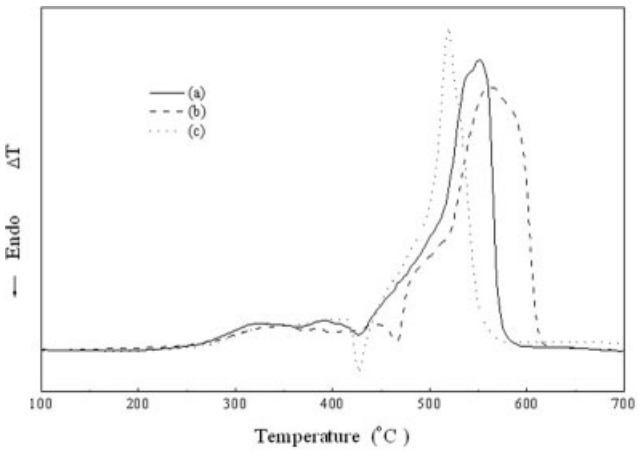

Figure 6 DSC curves at a heating rate of 10°C/min of (a) bisANER/MHHPA cured at 180°C, (b) bisANER/MHHPA cured at 200°C, and (c) bisANER/VCD/MHHPA cured at 180°C for 8 h.

TABLE III
Kinetic Parameters of the First Thermal Degradation Stage

Cured sample	Reaction order	Correlation coefficient	E (kJ/mol)	Log (A) (s^{-1})	Standard deviation
BisANER/MHHPA					
180°C	F_1	0.9911019	87.8	1.97	0.094
	F_2	0.1829882	0.36	−7.20	0.015
	F_3	0.0335535	10.96	−8.43	0.034
200°C	F_1	0.9830539	81.93	0.62	0.133
	F_2	−0.1661663	−0.69	–	–
	F_3	0.7318631	8.94	−8.68	0.073
BisANER/VCD/MHHPA					
180°C	F_1	0.9959989	94.8	4.16	0.050
	F_2	0.4999726	1.51	−8.33	0.015
	F_3	0.9235020	12.83	−8.04	0.031

stage are listed in Table III, and as shown in the Table III, the correlation values for different mechanisms are different. According to the principle that the probable mechanism has high correlation coefficient value, the probable mechanism functions of the thermal degradation reaction are deduced from the calculated results: first order. In addition, the degradation activation energy of bisANER/VCD/MHHPA is higher than that of the bisANER/MHHPA.

CONCLUSIONS

Curing reaction of bisANER with MHHPA studied using FTIR spectroscopy shows that the obvious structure changes involve the disappearance of epoxide groups, increase of hydroxyl and appearance of ester groups.

DSC studies show that the curing active energies of bisANER with MHHPA are lower than with 4,4′-diaminodiphenyl sulfone. The glass transition temperatures (T_gs) of bisANER/MHHPA increase with increasing temperature and time and leveled off a certain value.

Thermal degradation of bisANER/MHHPA network begins with the breaking of —OH, —CH_2—, —CH_3, OC—O, and C—O—C, etc. At higher degradation temperatures above 450°C, the carbonization or oxidation of the aromatic rings occurs. The degradation reaction takes place in two steps in dynamic air, and the kinetics analysis of bisANER/MHHPA determined with Coats–Redfern method shows that the probable mechanism is first-order reaction.

When vinyl cyclohexene dioxide (VCD) was used as a reactive diluent for bisANER, T_gs of the cured networks increase and the degradation temperature decrease slightly compared with the undiluted system.

References

1. Jain, P.; Choudhary, V.; Varma, I. K. Eur Polym J 2003, 39, 181.
2. Barton, J. M.; Harnerton, I.; Howlin, B. J.; Jones, J. R.; Liu, S. Y. Polymer 1998, 39, 1929.
3. Kaji, M.; Nakahara, K.; Ogami, K.; Endo, T. J Appl Polym Sci 1999, 74, 690.
4. Mailhot, B.; Morlat-Therias, S.; Ouahioune, M.; Gardette, J. L. Macromol Chem Phys 2005, 206, 575.
5. Mailhot, B.; Morlat-Therias, S.; Bussiere, P. O.; Gardette, J. L. Macromol Chem Phys 2005, 206, 585.
6. Nunez, L.; Fraga, F.; Nunez, M. R.; Villanueva, M. Polymer 2000, 41, 4635.
7. Luda, M. P.; Balabanovich, A. I.; Camino, G. J Anal Appl Pyrolysis 2002, 65, 25.
8. Duann, Y. F.; Liu, T. M.; Cheng, K. C.; Su, W. F. Polym Degrad Stab 2004, 84, 305.
9. Dyakonov, T.; Mann, P. J.; Chen, Y.; Stevenson, W. T. K. Polym Degrad Stab 1996, 54, 67.
10. Levchik, S. V.; Camino, G.; Luda, M. P.; Costa, L.; Muller, G.; Costes, B. Polym Degrad Stab 1998, 60, 169.
11. Guerrero, P.; Caba, K. D. L.; Valea, A.; Corcuera, M. A.; Mondragon, I. Polymer 1996, 37, 2195.
12. Davies, J.; Johncock, P.; Jones, D. A. Polymer 1999, 40, 4897.
13. Rose, N.; Bras, M. L.; Bourbigot, S.; Delobel, R.; Costes, B. Polym Degrad Stab 1996, 54, 355.
14. Levchik, S. V.; Camino, G.; Luda, M. P.; Costa, L.; Coates, B.; Henry, Y.; Muller, G.; Morel, E. Polym Degrad Stab 1995, 48, 359.
15. Goto, K.; Hayashi, S.; Saito, T.; Kaneko, T.; Mitani, K.; Wakabayashi, K.; Takagi, Y. U.S. Pat. 0,135,011 (2003).
16. Hooper, J. R.; Strother, R. K.; Fish, J.; Pawling, P. G.; Sauer, G. L. U.S. Pat. 6,040,397 (2000).
17. Taguchi, M.; Suzumura, Y.; Saitou, T.; Itou, A. U.S. Pat. 0,034,127 (2004).
18. Liu, Y. F.; Zhang, C.; Du, Z. J.; Li, H. Q. J Appl Polym Sci 2006, 99, 858.
19. Li, J. L.; Wo, S. K.; Zhang, Z. W.; Dong, J. W.; Yu, H. Thermosetting Resin (Chinese) 1998, 4, 30.
20. Jay, R. R. Anal Chem 1964, 36, 667.
21. Vatanparast, R.; Li, S. Y.; Lemmetyinen, H. J Appl Polym Sci 2001, 82, 2607.
22. Rocks, J.; George, G. A.; Vohwinkel, F. Polym Int 2003, 52, 1758.
23. Chen, L. W.; Fu, S. C.; Cho, C. S. Polym Int 1998, 46, 325.
24. Corcuera, M. A.; Mondragon, I.; Riccardi, C. C.; Williams, R. J. J. J Appl Polym Sci 1997, 64, 157.
25. Stevens, G. C. J Appl Polym Sci 1981, 26, 4259.
26. Ollier-Dureauly, V.; Gosse, B. J Appl Polym Sci 1998, 70, 1221.
27. Kissinger, H. E. Anal Chem 1957, 29, 1702.
28. Flynn, J. H.; Wall, L. A. Polym Lett 1966, 4, 232.
29. Ozawa, T. Bull Chem Soc Jpn 1965, 38, 1881.
30. Coats, A. W.; Redfern, J. P. Nature 1964, 201, 68.